

BEAM-BASED CALIBRATION OF LINEAR OPTICS MODEL OF NEWSUBARU

Y. Shoji,

LASTI, Himeji Institute of Technology, NewSUBARU/SPring-8, Kamigori, 678-1205, Japan

Abstract

We compared vertical linear optics of NewSUBARU with the present model. Quasi- π bumps were made to observe systematic differences between them. The next step was more careful investigations on non-symmetry of short local bumps. The measurements made it clear that there was systematic quadrupole differences at the long straight sections. A variation of strengths of vertical steering magnets would be explained by an interference with other magnets.

1 INTRODUCTION

Synchrotron radiation facility NewSUBARU [1] is a light source in the SPring-8 site and uses the 1.0 GeV linac as an injector. LASTI (Laboratory of Advanced Science and Technology for Industry) of Himeji Institute of Technology (HIT) is in charge of the construction and operation collaborating with SPring-8. The facility is financially supported by Hyogo prefecture.

The ring is a racetrack type with 6 bending cells, 2 dispersion free long straight sections (LSS) and 4 dispersion free short straight sections (SSS). Its circumference is 118.7m and it is now operated at 1 GeV. The bending cell is an achromatic triple bend, which middle bend is a small inverse bend to control the momentum compaction factor [1]. Typical betatron tunes are 6.30 and 2.23 for horizontal and vertical, respectively. Fig.1 shows 1/4 of the ring.

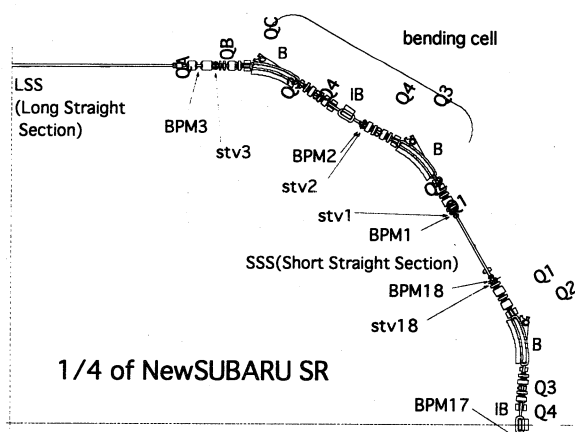


Figure 1: One quarter of NewSUBARU ring.

The model of NewSUBARU was far from a perfect. The betatron tunes are the most important parameters of linear optics; therefore we adjusted the parameter of Q-

magnets of the model so that the tunes of the model agree with those of the real machine, within an error. However the model was still not good enough. When we set parameters according to the model (1) linear dispersion was not zero at the straight sections, which should be zero, (2) local closed bumps using steering magnets was not closed. There are many ways of approaching to this problem. In this report we describe one of our trials, the test using vertical local bumps. We used 18 vertical steering magnets (stv) and 18 vertical beam position monitors (BPM).

2 QUASI-PI BUMP

2.1 Quasi-Pi Bump

Pi bump is a local bump orbit produced by a pair of steering magnets separated by just π in betatron phase. When the model is not accurate the local bump spills a C.O.D. wave out to the whole ring. An amplitude and a phase of the spilled give information on a strength and a location of an error. In NewSUBARU it was not easy to separate stv by just π . However we could apply the same analysis making quasi- π bumps.

We added the third stv to close the local bump but its strength was much weaker than those of the pair, so that the error of the third one less contribute to the spilled wave. We made 18 local bumps (closed in the model) in vertical direction and measured the spilled wave. Between the measurements of different local bumps we measured the C.O.D. with no bump. The data is analysed in the normalized phase space of betatron oscillation, where the π bump is a half cosine and the spilled wave is a simple sinusoidal wave. All sextupole magnets were turned off. In the analysis I also assumed symmetry of the ring.

2.2 Long Straight Sections (LSS)

There are southern and northern LSSs. However the spilled waves from two bumps at different but symmetric LSSs were roughly the same. Therefore we focus our discussion on the northern LSS between BPM11 and BPM14. The quasi- π bumps, which covered the northern LSS, and their spilled waves are shown in Fig. 2.

The error arrows of blue and pink bumps, the bottom two lines in Fig.2, are between BPM12 and BPM13, where there could be no error. The arrow should be separated into two arrows at the symmetric points, one between BPM10 and BPM11 and another between BPM12 and BPM13. The second arrow met the arrow of the brown bump. When these kicks are produced by the

same quadrupole error, their strengths should be proportional to the bump height, and they were. This means that there existed a stronger vertical defocusing (or weaker focusing) at LSS.

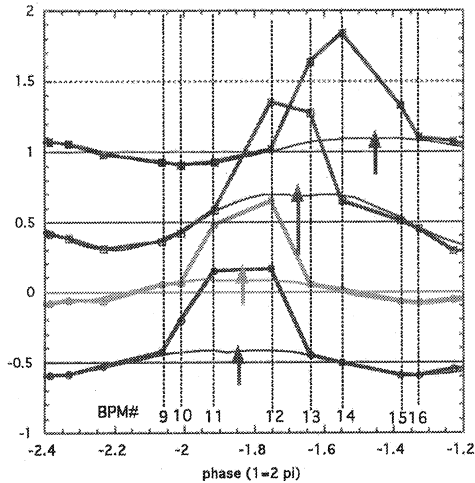


Figure 2: Quasi-pi bumps include the northern LSS. Thick lines with points present the measured C.O.D.s. Thin wavy lines show the fitted sinusoidal waves to the spilled waves. The arrows show locations and strengths of the estimated error kicks. The original colours of the bumps are blue, pink, brown and green from the bottom to the top

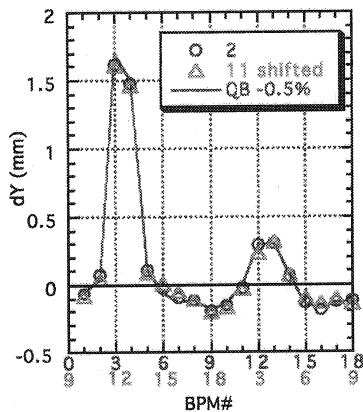


Figure 3: Spilled wave from the local quasi-pi bump at LSSs. The blue circles (southern LSS) and the red triangles (northern LSS) are the measured orbit. The solid black line is a calculated orbits assuming that the QB family is 0.5% weaker than the model.

The accuracy of the measurements was not high enough to identify the error magnet. Here we assume that the error magnet was QB (one of three families of Q magnets at LSS), which was most effective to change the vertical optics. Its strength error of 0.5% explains the spilled wave as shown in Fig. 3. The vertical tune in the model was

2.205 in the original model, and 2.170 in the weak QB model, where the measured tune was 2.155.

2.3 Bending Arcs

The quasi-pi bumps at the arcs (the sets of three bending cells) are shown in Fig. 4. Again the symmetry is clear then we analyse the western arc (from BPM4 to BPM12).

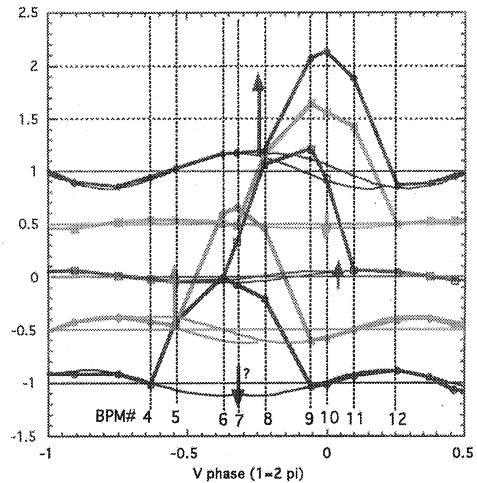


Figure 4: Quasi-pi bumps include the western arc. The meanings of points, lines and arrows are the same as those in Fig.2. The original colours of the bumps are blue, pink, brown, yellow and green from the bottom to the top

The error phase of the green bump at the top of Fig. 4 was on the steering (edge of the bump). This meant that the strength of stv8 or stv12 was wrong. The error steering was stv8 because stv12 was used also in the yellow bump but little spilled wave was observed. From investigations of the other bumps we could say all stv at the dispersive section (stv2, stv5, stv8, stv11, stv14 and stv17) were stronger than the others by 3~7%. Considering the error we concluded that all of them was 4.5% (we took the average) stronger than the others.

3 LOCAL BUMP

3.1 Short local bump

In the previous section we assumed the symmetry of the lattice. However when we made a narrow local bump using a set of 3 stv, spilled wave was considerable at some locations. A typical phase advance from the start to the end of the short bumps was $\pi/3 \sim 2\pi/3$.

3.2 stv-16

The spilled wave was large when we made a short bump at BPM13, BPM14 or BPM15, although the spilled wave was small when we made a bump at the symmetric points, BPM5, BPM6 or BP7.

We measured the same bump and spilled wave four times and the average of 4 data were used in the following analysis. We shifted the C.O.D. data of the short bump at BPM6 by a half turn and subtracted it from that at the symmetric point, BPM15. What we have got was a non-symmetric component. We also calculated non-symmetric components of the other 2 pairs. These non-symmetry were explained if stv16 is weaker than the model by 4.35% as shown in Fig.5.

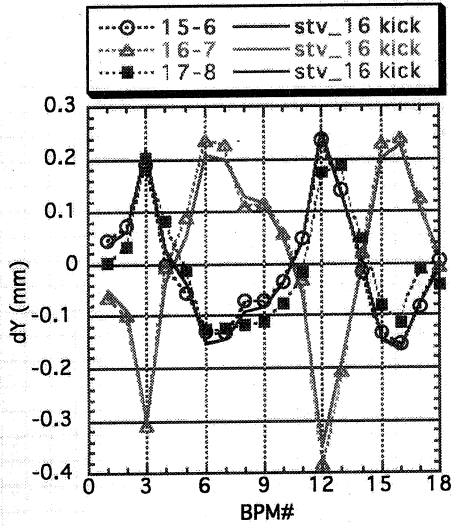


Figure 5. Non-symmetric components of the three short bumps. The lines with points show the observed. The solid lines are the calculated non-symmetric part assuming that stv16 is weaker than stv7 by 4.35%

4 MAGNET ARRANGEMENT

A possible reason of the reduction of the strength of stv might be an interference with other magnets. Fig.6 shows an arrangement of magnets around stv. The stv at the dispersive sections are in GROUP-A. The stv at LSS are in GROUP-B. The stv at SSS are in GROUP-C and -D.

The stv16 belongs to GROUP-D-2, which is a worst case. A sextupole magnet is very close to the stv on one side and a pulse bump magnet is set close on the other side.

In addition we expect that stv1 and stv18 (GROUP-D-1) may be weak. The observed non-symmetry including stv18 and stv1 was consistent with the reduction of their strength by 3.5%.

The result of section 3.2 is reasonable. The stv in GROUP-A are stronger than the others because they have much space to the magnets beside them.

5 CONCLUSION

The vertical focusing was weaker than the model at LSS. For more accurate calibration we need more measurements or the other kind of approach. Our study of beam-based calibration is still under way.

The interference between magnets reduced the strength of stv. This result may be confirmed by the field measurement.

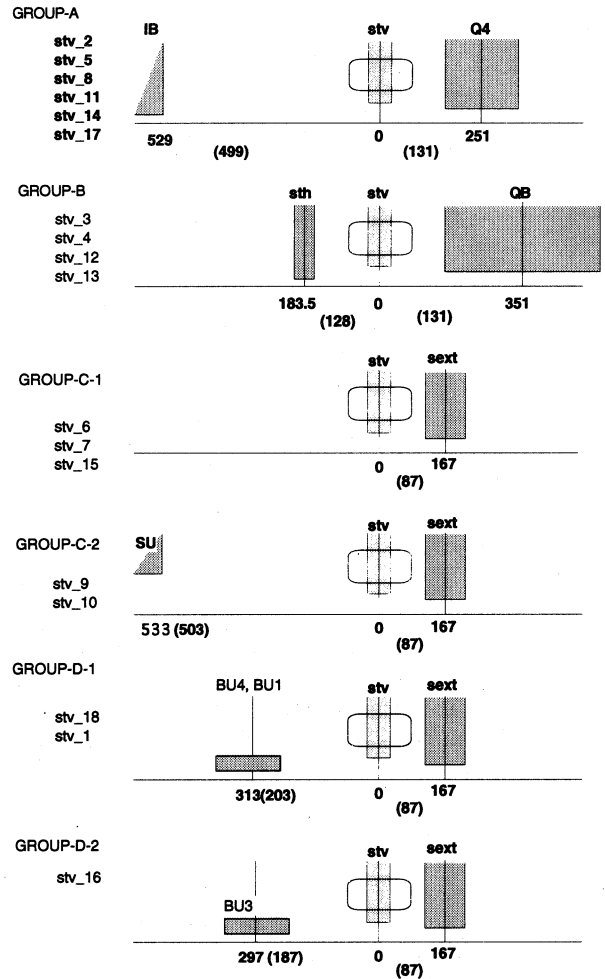


Figure 6: Lay out of magnets near stv. They are grouped according to the magnets set beside them. The numbers below the lines are the positions of the magnet centre in mm. The numbers in the brackets are the distance between the yoke faces. A small gap between a shaded yoke and the horizontal line is a bore radius. A rounded square overlapping with the stv yoke is a coil.

6 ACKNOWLEDGEMENT

I thank members of the accelerator group of LASTI and SPring-8 for their help. Especially Dr. K. Kumagai gave me a suggestion on the reduction of strength of magnets.

REFERENCES

- [1] S. Hashimoto, *et al.*, Trans. Materials Research Soc. Japan, **26**[2], 783-786 (2001).